



Article

Genome-Wide Analysis and Expression Profiling of Glutathione Reductase Gene Family in Oat (*Avena sativa*) Indicate Their Responses to Abiotic Stress during Seed Imbibition

Ming Sun, Shoujiang Sun , Zhicheng Jia , Wen Ma, Chunli Mao, Chengming Ou, Juan Wang, Han Zhang, Liu Hong, Manli Li, Shangang Jia and Peisheng Mao *

Forage Seed Laboratory, College of Grassland Science and Technology, China Agricultural University, Beijing 100193, China

* Correspondence: maops@cau.edu.cn



Citation: Sun, M.; Sun, S.; Jia, Z.; Ma, W.; Mao, C.; Ou, C.; Wang, J.; Zhang, H.; Hong, L.; Li, M.; et al. Genome-Wide Analysis and Expression Profiling of Glutathione Reductase Gene Family in Oat (*Avena sativa*) Indicate Their Responses to Abiotic Stress during Seed Imbibition. *Int. J. Mol. Sci.* **2022**, *23*, 11650. <https://doi.org/10.3390/ijms231911650>

Academic Editor: Yong-Hwan Moon

Received: 11 August 2022

Accepted: 23 September 2022

Published: 1 October 2022

Publisher's Note: MDPI stays neutral with regard to jurisdictional claims in published maps and institutional affiliations.



Copyright: © 2022 by the authors. Licensee MDPI, Basel, Switzerland. This article is an open access article distributed under the terms and conditions of the Creative Commons Attribution (CC BY) license (<https://creativecommons.org/licenses/by/4.0/>).

Abstract: Abiotic stress disturbs plant cellular redox homeostasis, inhibiting seed germination and plant growth. This is a crucial limitation to crop yield. Glutathione reductase (GR) is an important component of the ascorbate-glutathione (AsA-GSH) cycle which is involved in multiple plant metabolic processes. In the present study, GRs in *A. sativa* (*AsGRs*) were selected to explore their molecular characterization, phylogenetic relationship, and RNA expression changes during seed imbibition under abiotic stress. Seven *AsGR* genes were identified and mapped on six chromosomes of A, C, and D subgenomes. Phylogenetic analysis and subcellular localization of *AsGR* proteins divided them into two sub-families, *AsGR1* and *AsGR2*, which were predicted to be mainly located in cytoplasm, mitochondrion, and chloroplast. *Cis*-elements relevant to stress and hormone responses are distributed in promoter regions of *AsGRs*. Tissue-specific expression profiling showed that *AsGR1* genes were highly expressed in roots, leaves, and seeds, while *AsGR2* genes were highly expressed in leaves and seeds. Both *AsGR1* and *AsGR2* genes showed a decreasing-increasing expression trend during seed germination under non-stress conditions. In addition, their responses to drought, salt, cold, copper, H₂O₂, and ageing treatments were quite different during seed imbibition. Among the seven *AsGR* genes, *AsGR1-A*, *AsGR1-C*, *AsGR2-A*, and *AsGR2-D* responded more significantly, especially under drought, ageing, and H₂O₂ stress. This study has laid the ground for the functional characterization of GR and the improvement of oat stress tolerance and seed vigor.

Keywords: *A. sativa*; glutathione reductase; abiotic stress; seed imbibition; qPCR

1. Introduction

Reactive oxygen species (ROS) are key regulators of plant growth and development throughout the whole plant life cycle [1,2]. Without stresses, ROS in the organism maintain the dynamic equilibrium by various antioxidative defense mechanisms [3,4]. The equilibrium of ROS-producing and ROS-scavenging can be changed under stressful conditions, which thus leads to the excessive accumulation of ROS, lipid peroxidation, protein oxidation, and nucleic acid damage [4]. Recent studies have substantiated that ROS play a pivotal role in the regulation of seed germination, dormancy, and longevity [1,2,5]. However, adverse seed storage and germination conditions often lead to ROS accumulation, and inhibit germination and normal seedling establishment. The major sources of ROS production in plants are chloroplasts, mitochondria, peroxisome, apoplast, etc. [3]. In orthodox seeds, the mitochondrion is the main source of ROS (especially in seed germination) [6]. Therefore, alleviating the excessive accumulation of ROS and maintaining the dynamic balance of ROS are key to coping with the adverse environment.

In plants, the ascorbate-glutathione (AsA-GSH) cycle as an antioxidant system, which involved enzymatic and non-enzymatic antioxidants, plays a vital role in detoxifying

ROS [7]. Glutathione (GSH; γ -glutamyl-cysteinyl-glycine), an omnipresent low-molecular-weight thiol compound, is a strong non-enzymatic antioxidant and an essential metabolite with multifunction in plants [8,9]. It participates in various biological processes, including antioxidant defense, redox signaling, xenobiotics detoxification, etc. [8,9]. Due to the nucleophilic nature of their cysteine residues, GSH can be converted to oxidized glutathione disulfide (GSSG). Typically, the intracellular GSH concentration is kept at the millimole levels, and up to 90% GSH is in its reduced form under normal conditions [8]. Glutathione reductase (GR, EC 1.6.4.2) belongs to the NADPH-dependent oxidoreductase group of flavoproteins and plays an important role in catalyzing the reduction of GSSG to GSH using NADPH as electron donor in eukaryotes and prokaryotes [7,10]. The redox balance of the GSH/GSSG couple is essential for maintaining seed vigor and normal germination, and the increase of endogenous and exogenous GSH is beneficial for seed vigor improvement under stress [11–13]. The expression levels of GR genes can be significantly induced by unfavorable conditions. The deletion or down-regulation of GR genes would lead to the decrease of seed vigor [14]. Moreover, GR activity increases during germination both in embryo and endosperm. These suggest that GSH and GR play a considerable role in the maintenance of the intracellular redox balance and biological functions.

In plants, GRs are mainly localized in chloroplast, mitochondria, and cytosol [10]. Previous works have classified GR proteins into two clades of GR1 and GR2 on the basis of the presence of N-terminal extension. GR1 is a shorter cytosolic enzyme, and GR2 representing the elongated organellar proteins can target the GR proteins in both mitochondria and chloroplast [15]. NADPH binding domain, FAD binding domain, and the interface domain binding the two subunits of GR proteins are identified in GR proteins. GRs have been suggested to play a central role in maintaining the reduced GSH pool and improving abiotic and biotic stress resistance [10,16,17]. The localizations where GR is active are also the sources of ROS, such as chloroplasts and mitochondria. Oxidative stress caused by drought, temperature, heavy metals, salinity, and hydrogen peroxide can induce changes of GR gene expression and GR enzyme activity [10,18,19]. Overexpression of GRs improved the stress resistance in transgenic plants, and the deletion of GRs led to the decrease of antioxidant capacity [14,20–22].

The GR protein encoded by a small gene family has been described in many crops and model plants, such as *Arabidopsis thaliana*, *Brassica juncea*, *Brassica rapa*, *Oryza sativa*, *Populus trichocarpa*, *Aegilops tauschii*, and *Triticum aestivum* [15,17,23,24]. The genome-wide identification of GRs, and characterizing its structure and function, would be useful for future functional and mechanism studies on GR proteins. In addition, RNA-seq and quantitative real-time PCR (qPCR) analysis of GR genes indicated that they strongly responded to abiotic and biotic stresses and plant hormones [17,18]. Typically, two or three GRs are found in the above reported species. Recently, seven GR genes were identified in the allohexaploid genome (AABBDD) of bread wheat [24]. Oats (*Avena sativa*) are also an allohexaploid species (AACCCDD, $2n = 6x = 42$) and rank sixth in world cereal production due to high nutritional and medicinal value and broad distributions [25]. The identification of essential gene families, especially antioxidant gene families, has not been carried out in oats, as the chromosome-scale reference genome was recently available (<https://wheat.pw.usda.gov/GG3/graingenes-data-downloads>, accessed on 24 November 2021) [26,27]. In addition, the central roles of GSH and GRs in seed vigor maintenance and seed germination have been demonstrated, but the divergent roles of different GR isoforms in seed germination under stress have not been reported. The aim of this study was to identify *A. sativa* GR genes in the whole genome level, and perform analysis of gene and protein structure, in silico subcellular localization prediction, and biochemical characterization. Moreover, the relative expressions of these members in response to the treatments of drought, salt, cold, CuSO_4 , H_2O_2 , and ageing were compared by qPCR, in seed imbibition. This work can be utilized in future genetic improvement of *A. sativa* for stress tolerance and seed vigor.

2. Results

2.1. Identification and Chromosomal Mapping of GR Genes

A total of thirteen GR genes were identified in *A. sativa* and its possible ancestors, namely *A. longiglumis* and *A. insularis*. The diploid *A. longiglumis* (AA) consisted of two GR genes which were distributed in chromosome 5A and 6A, respectively (Figure 1B). Four GR genes were identified from tetraploid *A. insularis* (CCDD), and they were distributed in chromosomes of 1D, 4C, 6C and 6D (Figure 1C). However, seven AsGR genes located at chromosomes of 1D, 4A, 4C, 6A, 6C and 6D were identified from allohexaploid *A. sativa* (Figure 1A). According to homologous relationships with the two *Arabidopsis* GR proteins and their sub-genomic locations, *A. sativa* GR genes were clustered into two homologous groups AsGR1 and AsGR2, and named as AsGR1-A, AsGR1-C, AsGR1-D, AsGR2-A, AsGR2-C1, AsGR2-C2, and AsGR2-D. *A. longiglumis* GR genes were named as AIGR1-A and AIGR2-A, and *A. insularis* GR genes were named as AiGR1-C, AiGR1-D, AiGR2-C, and AiGR2-D.

Chromosome mapping results showed the number of AsGR genes were one more than the six ones by combining its diploid (*A. longiglumis*) and tetraploid (*A. insularis*) progenitors. Chromosome 4C of *A. insularis* had a single GR gene, while chromosome 4C of *A. sativa* consisted of two AsGR genes, which revealed the gain of one more GR gene during evolution. Both chromosome 5 and 6 of AA progenitor had one GR gene, respectively, while there is no GR gene in chromosome 5A of *A. sativa*. Instead, chromosome 4A gained a AsGR gene. This indicated an occurrence of a recombination between different chromosomes during evolution. Moreover, most of the AsGR genes are distributed at the ends of chromosomes, which also suggests their potential translocation between different chromosomes.

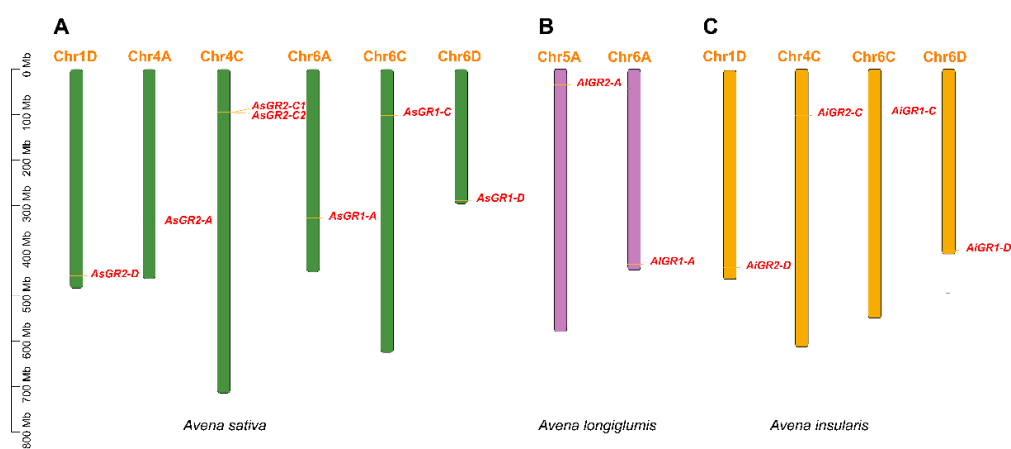


Figure 1. Chromosomal mapping of GR genes in *A. sativa* (A), *A. longiglumis* (B), and *A. insularis* (C). The chromosome number is denoted on the top of each chromosome. The scale is marked in megabases (Mb).

2.2. Physico-Chemical Properties of AsGR Family

We looked into the physico-chemical properties of AsGR proteins, including the amino acid composition, molecular weight, theoretical isoelectric point (pI), instability index, and negatively and positively charged residues. The molecular weight of AsGRs was ranging from 34.718 to 93.097 kDa, which is in accordance with the amino acid length from 321 (AsGR2-C2) to 853 (AsGR1-D). All three AsGR1 members showed slightly acidic pI, while AsGR2 members showed divergent pI. AsGR2-C2 showed acidic pI (5.34), AsGR2-C1 and AsGR2-D showed nearly neutral pI (6.93), and AsGR2-A had alkalic pI (9.59). The instability index prediction showed that AsGR1 proteins and AsGR2-C2 were stable (Instability index < 40), while AsGR2-C1, AsGR2-D, and AsGR2-A were classified as unstable ones with high instability index. Additionally, almost all of the AsGR proteins were found to be rich in negatively charged residues, except for AsGR2-A (Table 1).

Table 1. Physico-chemical properties of GR family in *A. sativa*.

Gene Names	Gene ID	Chromosomal Location	Number of Amino Acids	Molecular Weight	pI	Instability Index	Negatively/Positively Charged Residues
AsGR1-A	AVESA.00001b.r1.6Ag0001934.1	6A: 328352411..328361762	533	57.176	5.96	28.52	66/60
AsGR1-C	AVESA.00001b.r1.6Cg0000969.1	6C: 102116290..102123495	498	53.430	5.82	25.74	62/56
AsGR1-D	AVESA.00001b.r1.6Dg0001672.1	6D: 288925140..288934590	853	93.097	6.00	29.34	115/105
AsGR2-A	AVESA.00001b.r1.4Ag0002233.1	4A: 337954968..337961977	798	87.477	9.59	53.87	90/123
AsGR2-C1	AVESA.00001b.r1.4Cg0001182.1	4C: 94048476..94053156	551	59.450	6.93	40.76	62/61
AsGR2-C2	AVESA.00001b.r1.4Cg0001191.1	4C: 95512612..95515711	321	34.718	5.34	35.01	41/32
AsGR2-D	AVESA.00001b.r1.1Dg0003199.1	1D: 455767235..455771855	543	58.772	6.93	42.23	62/61

2.3. Phylogenetic Analysis and In Silico Subcellular Localization of GR Proteins

To understand the phylogenetic relationship and classification of GR proteins, we constructed a phylogenetic tree with the protein sequences of GRs from *A. sativa*, *A. longiglumis*, and *A. insularis*, as well as known GRs classified from *Arabidopsis*, rice, and bread wheat (Figure 2). All GR proteins are divided into two well-differentiated clades. Clade I contained AsGR1, AlGR1, AiGR1, AtGR1, OsGR2, and TaGR2 proteins, and Clade II consisted of AsGR2, AlGR2, AiGR2, AtGR2, OsGR1, OsGR3, and TaGR1 proteins. Both *A. sativa* and bread wheat are allohexaploid and have the same number of GRs, but there are three AsGRs and four TaGRs in Clades I, while four AsGRs and three TaGRs in Clade II. The distribution and classification of the GR members from A and D subgenomes are identical in the two species, but the classification is different in the unique B or C subgenome. AsGR2-C1 and AsGR2-C2 with close proximity on chromosome 4C were in the same clade, which indicated that AsGR2-C1 and AsGR2-C2 may be a result of expansion of tandem replication.

Additionally, the grouping of AsGR proteins is highly associated with their in silico subcellular localization prediction results. AsGR1 proteins were predicted to be localized in the cytosol, and AsGR2 proteins were mainly localized in the plastid and mitochondria (Table 2). The results are consistent with the experimental subcellular localization of AtGRs and OsGRs and in silico prediction of TaGRs. Taken together, phylogenetic analysis and in silico subcellular localization indicated that GR, as an important oxidoreductase, has formed two main isoforms that may play specific roles in different tissues and under different environmental conditions. Therefore, it is of great significance to precisely regulate cellular GSH pool during plant development and stress conditions.

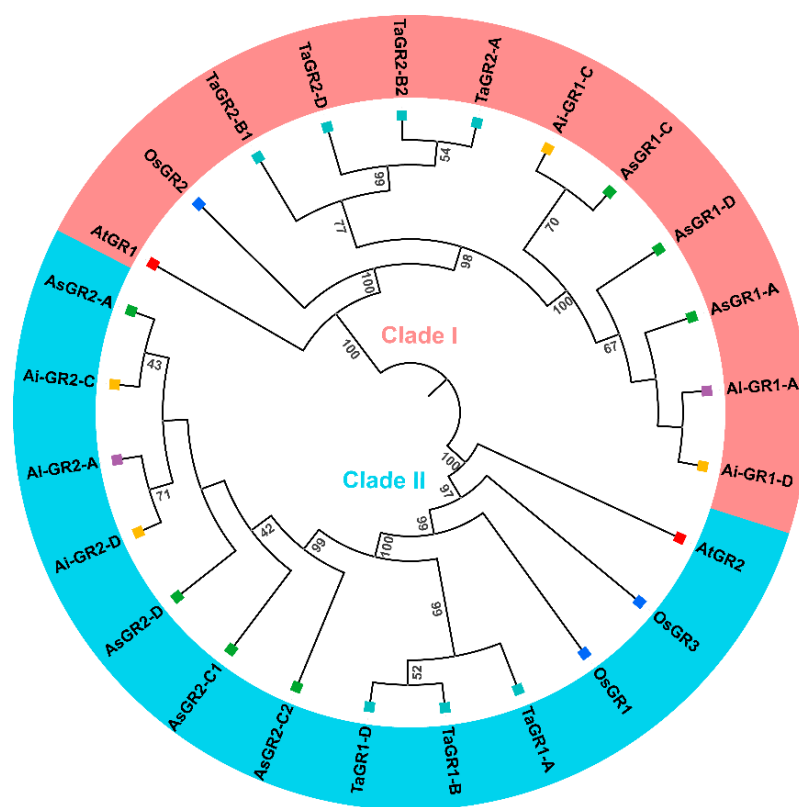


Figure 2. Phylogenetic relationships of GR proteins. The phylogenetic tree based on GR sequences from *A. sativa* (green), *A. longiglumis* (purple), *A. insularis* (orange) *Arabidopsis* (red), rice (blue), and bread wheat (turquoise) was constructed using MEGA v6 with the neighbor-joining (NJ) method, and the bootstrap test replicate was set as 10,000 times.

Table 2. In silico subcellular localization prediction of GR proteins.

Species	Proteins	CELLO	WoLF PSORT	Plant-mPloc
<i>A. sativa</i>	AsGR1-A	Cytoplasm	Cytoplasm	Chloroplast. Cytoplasm
	AsGR1-C	Cytoplasm	Cytoplasm	Chloroplast. Cytoplasm
	AsGR1-D	Cytoplasm	Cytoplasm	Chloroplast. Cytoplasm
	AsGR2-A	Mitochondrion	Chloroplast	Chloroplast. Cytoplasm. Mitochondrion
	AsGR2-C1	Chloroplast	Chloroplast	Chloroplast. Cytoplasm. Mitochondrion
	AsGR2-C2	Cytoplasm	Cytoskeleton	Chloroplast. Cytoplasm. Mitochondrion
	AsGR2-D	Chloroplast	Chloroplast	Chloroplast. Cytoplasm. Mitochondrion
<i>A. longiglumis</i>	AlGR1-A	Cytoplasm	Cytoplasm	Chloroplast. Cytoplasm
	AlGR2-A	Chloroplast	Chloroplast	Chloroplast. Cytoplasm. Mitochondrion
<i>A. insularis</i>	AiGR1-C	Cytoplasm	Cytoplasm	Chloroplast. Cytoplasm
	AiGR1-D	Cytoplasm	Cytoplasm	Chloroplast. Cytoplasm
	AiGR2-C	Chloroplast	Chloroplast	Chloroplast. Cytoplasm. Mitochondrion
	AiGR2-D	Chloroplast	Chloroplast	Chloroplast. Cytoplasm. Mitochondrion

2.4. Motif Pattern and Gene Structure Analysis of AsGR Members

A total of 15 conserved motifs were detected in 7 AsGR proteins, of which motif 1, 2, 3, 5, 7, and 9 were shared by all AsGRs. AsGR2-C2 has the minimum amino acid sequence length and motif number, which is different from the other three AsGR2 proteins. Motif 12 is specific to AsGR2 and is replaced by motif 13 in AsGR1. In addition to AsGR2-C2, motif 10 is also unique to AsGR2. Motif 14 is common in AsGRs, but it is at the N- and C-terminals in AsGR1 and AsGR2, respectively. Motif 15 exists in only two members (at the C-terminus of AsGR1-D, and at the N-terminus of AsGR2-A) (Figure 3A,B).

Gene structure analysis showed that most genes had multiple exons and introns. The number of exons of *AsGR1* genes is more than that of *AsGR2* genes, and the maximum number is 19 in *AsGR1-D*. The longest exon is also present in *AsGR1-D* at the 3' end of the gene. Although the motif distribution pattern of GR protein is basically the same, the structure of most *AsGR* genes is different. *AsGR2-C1* and *AsGR2-D* have similar gene structure and motif distribution, indicating that they may have the same ancestors and similar functions (Figure 3C).

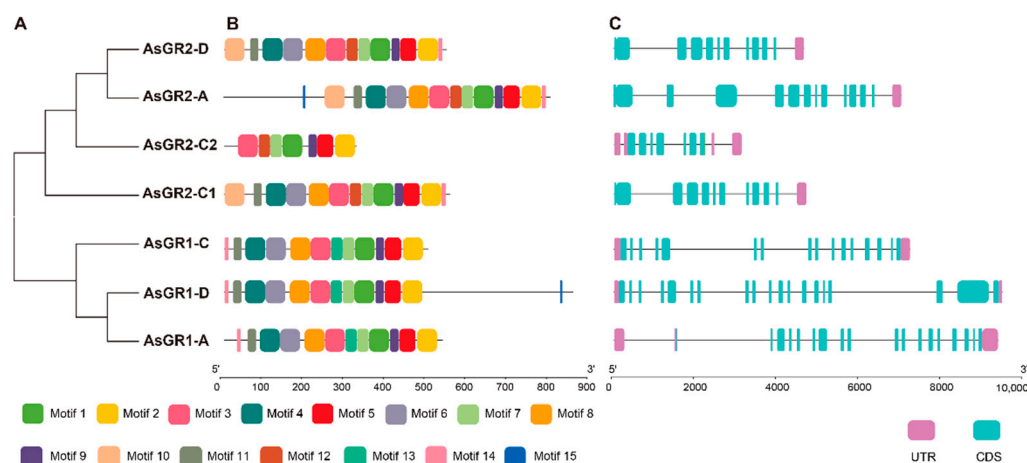


Figure 3. The motif pattern and gene structure of GR members in *A. sativa*. (A) Phylogenetic clustering showed that AsGR members were grouped into two subfamilies. (B) The schematics represents the motif patterns of AsGR proteins. Different colored boxes indicated the fifteen different MEME-motifs. (C) Gene structures of the seven *AsGR* genes. Pink boxes indicate untranslated regions (UTR), and exons and introns are indicated by turquoise boxes and black lines, respectively.

2.5. Structural Analysis and Homology Modelling of AsGR Members

Multiple sequence alignment of GR protein in *A. sativa* and *Arabidopsis* showed that both AsGR1 and AsGR2 members had highly conserved reactive disulfide bridge domain, NADPH binding domain, FAD binding domain and GSSG binding domain (Figure 4). The conserved disulphide bridge domain containing signature (GGTCV[I/L]RGCVPKK[I/L]LVY) has two active cysteine residues, which participate in the transfer of reducing equivalent from FAD to glutathione. In NADPH binding site, two conserved arginine residues were found for NADPH binding. Amino acid substitutions between AsGR1 and AsGR2 were common. Amino acid substitutions between GR1 and GR2 shared in *A. sativa* and *Arabidopsis* were found in active site, NADPH binding site and GSSG binding site, including I, L, K, Q, P, V, S, and T. There are specific substitutions of AsGR1 and AsGR2, with substitutions in the active site (H/V), the NADPH binding site (E/P), the FAD binding site (N/S), and the GSSG binding site (A/S), respectively. But the substitution of S and A in the GSSG binding sites of *Arabidopsis* was just the opposite. In addition, in *Arabidopsis* and *A. sativa*, the N-terminal targeting signal peptide for chloroplastic isoforms are not conserved, but the targeting signal peptide for cytosolic isoforms are relatively conserved ([I/Q]DG[T/S]K) (Figure 4).

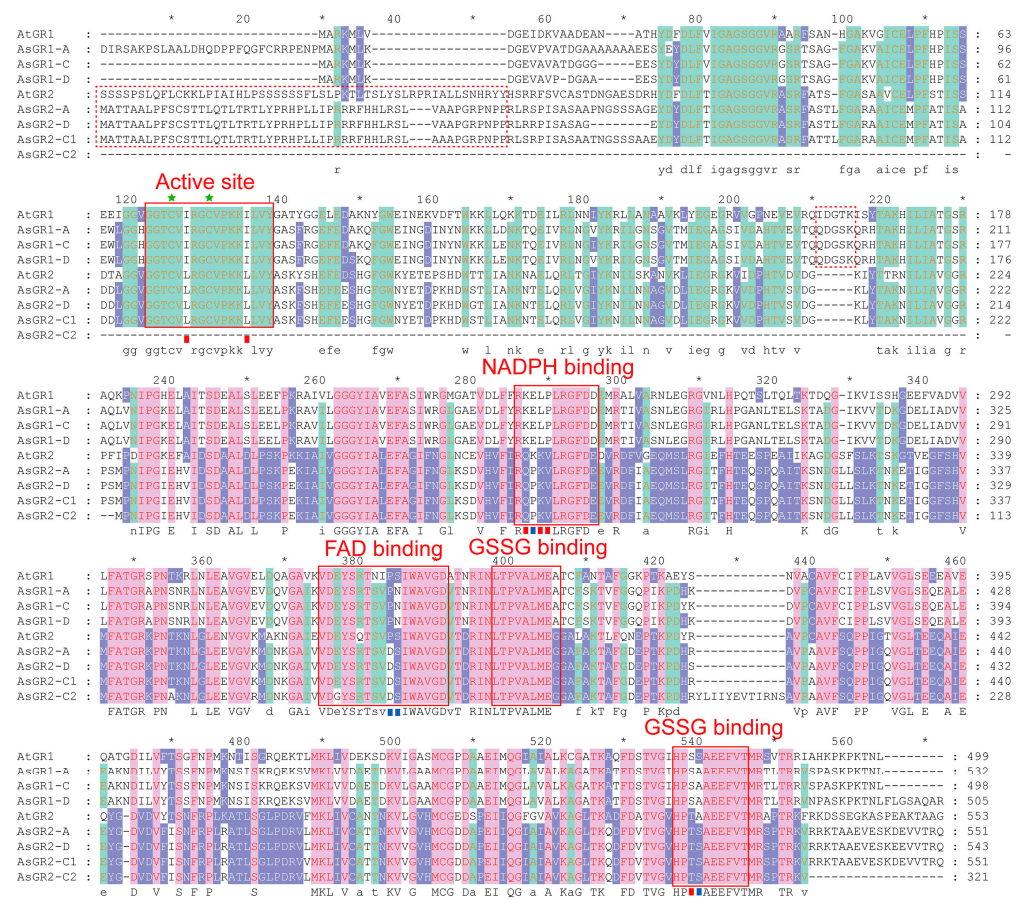


Figure 4. Multiple sequence alignments of AsGR and AtGR proteins. The active site domain, NADPH-binding domain, FAD binding domain, and GSSG binding domain in GR proteins are indicated with a red solid box. The targeting signal peptide for chloroplastic and cytosolic isoforms are shown in red dotted box. Green stars show the cysteine residues involved in catalytic site. Red squares highlight the amino acid substitutions in the GR specific structural domains of cytosolic and chloroplastic GRs. Blue squares highlight the amino acid substitutions in the GR specific structural domains of in AsGRs only.

The three-dimensional structure of seven AsGR family members were modelled using Phyre2 server. Predicted models were based on the reported templates to heuristically maximize the identity and confidence score for the tested sequences. In AsGR proteins, the mainly predicted secondary structures were α -helix (28–33% in each AsGR) and β -strands (23–30% in each AsGR). All AsGR sequences showed high confidence of 100% with the template. In addition, about 46–48% identity was demonstrated between AsGR proteins and the template, suggesting that the predicted AsGRs models had extremely high accuracy (Figure 5).

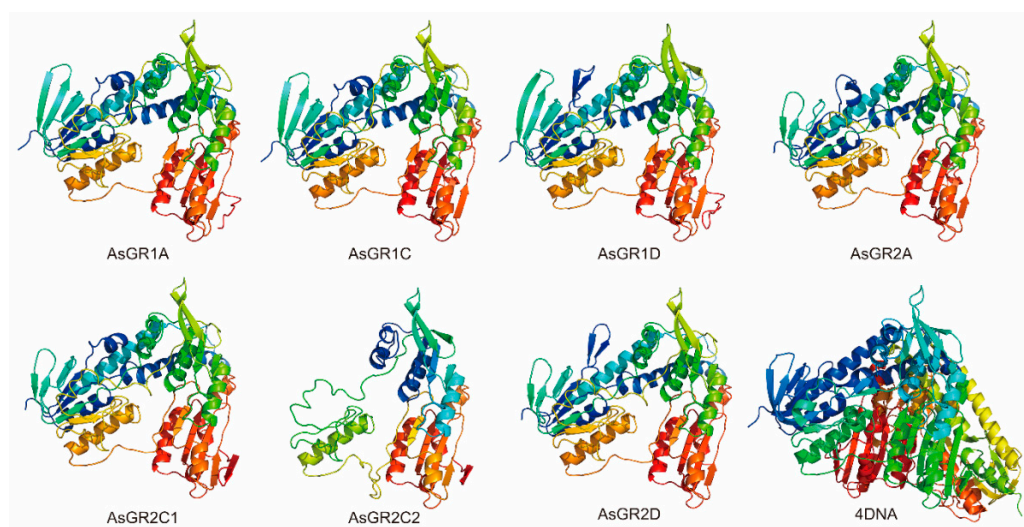


Figure 5. Three-dimensional structure of putative GR proteins from *A. sativa* generated through homology modelling. All AsGR proteins were modelled using the crystal structure of putative glutathione reductase from *Sinorhizobium meliloti* 1021 (PDB: 4DNA) chain A as template.

2.6. Identification of Cis-Elements in the Promoter Region of AsGR Genes

The common *cis*-acting element CAAT-box and the core promoter element TATA-box were found to be widely distributed in the promoter region of the *AsGR* genes (data not show). The other *cis*-acting elements are mainly related to hormone responsiveness, anaerobic induction, defense and stress responsiveness and light responsiveness (Figure 6). Hormone responsiveness elements mainly comprised of *cis*-elements associated with ABA, GA, MeJA, SA, and IAA responses. These hormone responsiveness elements appear to be specific for *AsGR1* and *AsGR2*. The stress responsiveness elements are mainly related to drought, low temperature, and defense and stress response. In addition, there are some other elements including MYBHv1 binding site (*AsGR2-D*, *AsGR2-A*, *AsGR2-C2*, *AsGR1-A*, and *AsGR1-C*), zein metabolism regulation (*AsGR2-D*, *AsGR2-A*, *AsGR2-C1*, and *AsGR1-C*), MYB binding site involved in drought-inducibility (*AsGR2-C1*, *AsGR2-A*, *AsGR2-C2*, *AsGR1-A*, and *AsGR1-D*), meristem expression (*AsGR2-C2*, *AsGR1-A*, and *AsGR1-D*), and circadian regulation (*AsGR2-C1*) (Figure 6).

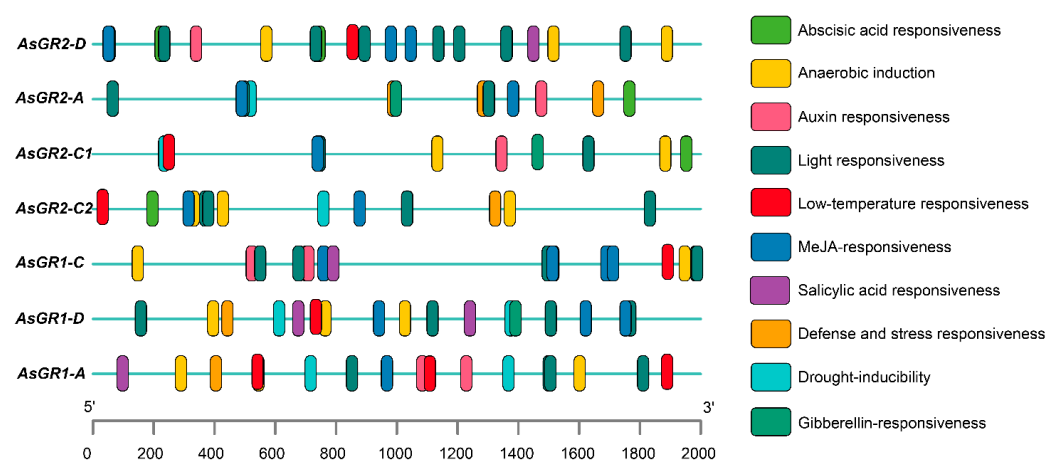


Figure 6. *Cis*-regulatory elements in the promoters of *AsGR* gene family.

2.7. Tissues Specific Expression Analysis of AsGR Genes

The expression of *AsGR1* and *AsGR2* genes varied considerably in different tissues (Figure 7). The expression pattern of *AsGR1-A* and *AsGR1-C* was basically identical, and significantly different from that of *AsGR1-D*. *AsGR1-A* and *AsGR1-C* were highly expressed

in dry seeds, roots, old leaves, and lemmas, while *AsGR1-D* was highly expressed in dry seeds, seeds, leaves, lemmas, and late developing seeds but was with low level in roots. The expression patterns of *AsGR2-C1*, *AsGR2-C2*, and *AsGR2-D* are generally consistent, which showed the highest expression level in young leaves, followed by old leaves, lemmas and dry seeds, and the lowest in roots. The expression of *AsGR2-A* was the highest in dry seeds, followed by leaves and lemmas. On the whole, *AsGR* genes have relatively high expression in leaves and dry seeds, indicating that they may play a role in maintaining leaf function and seed vigor (Figure 7).

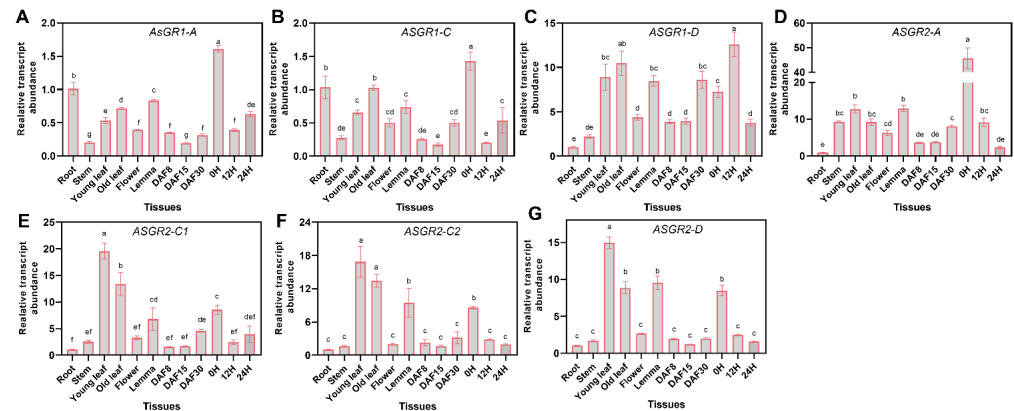


Figure 7. Expression profiling of *AsGR1-A* (A), *AsGR1-C* (B), *AsGR1-D* (C), *AsGR2-A* (D), *AsGR2-C1* (E), *AsGR2-C2* (F), and *AsGR2-D* (G) genes in different tissues of *A. sativa* by qPCR. The relative expression was calculated using transcription level of root as reference. Seeds imbibed for 0 h, 12 h, and 24 h in germination phases were marked as 0 H, 12 H, and 24 H, respectively. Developing seeds at 8, 15, and 30 days after flowering were marked as DAF8, DAF15, and DAF30, respectively. The lower-case letters (a–f) represent statistical significance among different tissues and the vertical bars represent the \pm SEM at $p < 0.05$ level for three replicates. The mean values sharing same letters, obtained from Duncan test, are not different significantly.

2.8. Expression Analysis of *AsGR1* Genes in Seed Imbibition under Stress

Under the non-stress and stress treatments, *AsGR1-A* and *AsGR1-C* showed firstly decreasing and then increasing expression trends, while *AsGR1-D* mainly presented two expression peaks during imbibition (0–72 h). The expression of *AsGR1-C* in aged seeds was significantly down-regulated in dry seeds ($p < 0.05$), which may cause the destruction of redox balance in the early imbibition of *A. sativa* seeds. *AsGR1-A* expression was up-regulated at most imbibition time under stress compared with the control. After 6 h of imbibition, the expression of *AsGR1-A* significantly increased in cold, PEG, salt, CuSO_4 and H_2O_2 treatments. Under PEG and salt treatments, *AsGR1-A* expression increased significantly after 24–72 h imbibition. Under H_2O_2 treatment, the expression of *AsGR1-A* was the highest in dry seeds and seeds treated for 36 and 72 h. The expression of *AsGR1-A* in aged seeds was lower compared with other treatments at 24 h imbibition (Figure 8A). *AsGR1-C* showed a minor response to CuSO_4 and H_2O_2 treatments, while it strongly responded to salt treatment at the early imbibition stage (6 h and 12 h). After 72 h imbibition, the expression of *AsGR1-C* was also significantly induced under PEG stress ($p < 0.05$) and in aged seeds ($p < 0.01$) (Figure 8B). *AsGR1-D* was significantly changed after all of the treatments. It was highly up-regulated under H_2O_2 and D30 treatment during imbibition (6–72 h). The highest expression level was present at 36 h under H_2O_2 treatment. Cold treatment also could induce the expression of *AsGR1-D* at 6–36 h. However, the expression of *AsGR1-D* was lower at 72 h imbibition under cold, PEG, salt and CuSO_4 treatments than control (Figure 8C). In addition, the expression level of *AsGR1-A* and *AsGR1-D* in aged non-imbibition seeds was not significantly changed (Figure 8A,C).

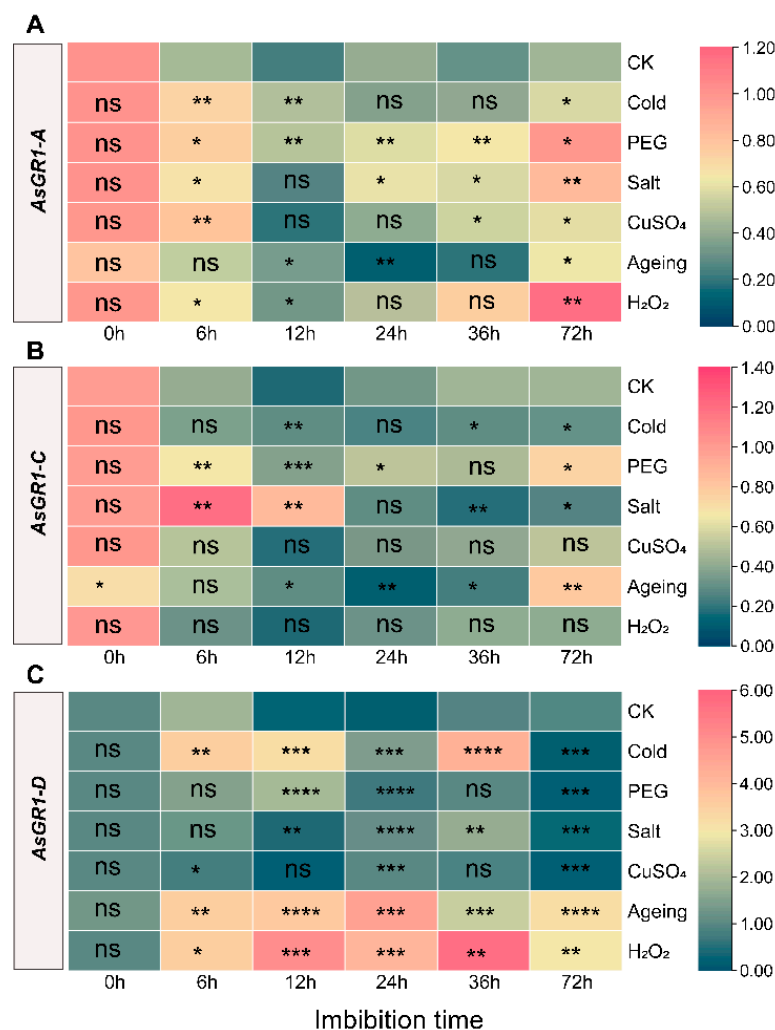


Figure 8. Expression profiling of *AsGR1-A* (A), *AsGR1-C* (B), and *AsGR1-D* (C) during seed imbibition under stress by qPCR. The relative expression was calculated using transcription level of dry seed (0 h) of CK as reference. The significant expression change in comparison to normal conditions (CK) has been calculated using Student's *t* test. * indicates a significant difference at $p < 0.05$; ** indicates a significant difference at $p < 0.01$; *** indicates a significant difference at $p < 0.001$; **** indicates a significant difference at $p < 0.0001$; ns represents not significant.

2.9. Expression Analysis of *AsGR2* Genes in Seed Imbibition under Stress

The response of *AsGR2* genes to different stress treatments is also different, and most of them have strong response in the early imbibition stage, except for *AsGR2-C2* (Figure 9). After ageing treatment, *AsGR2-C2* and *AsGR2-D* were significantly down-regulated compared with control in non-imbibition seeds ($p < 0.05$) (Figure 9). *AsGR2-A* was considerably induced by various stresses. In detail, among the treatments, PEG, H₂O₂ and ageing treatments significantly induced the expression of *AsGR2-A* gene within 72 h of imbibition. The expression of *AsGR2-A* was up-regulated during 6–36 h imbibition, but was down-regulated at 72 h. Under CuSO₄ and salt treatment, *AsGR2-A* was also significantly changed during 24–72 h (Figure 9A). *AsGR2-C1* was significantly induced for high expression in the beginning of seed imbibition (6 h) under stress treatments, especially PEG and D30 treatments. After 12 h imbibition, *AsGR2-C1* abundance in aged seeds was still in a higher level (Figure 9B). During the imbibition under non-stress and stress conditions, *AsGR2-C2* abundance decreased firstly and then increased. Ageing treatment markedly changed the expression patterns of *AsGR2-C2* during imbibition. *AsGR2-C2* levels in aged seeds was higher than that of the control during 12–24 h. Under PEG treatments,

AsGR2-C2 was up-regulated during 12–36 h, but it was significantly down-regulated at 72 h (Figure 9C). *AsGR2-D* significantly responded to most of the stresses, especially under PEG, salt, ageing and H₂O₂ treatments. *AsGR2-D* expression was strongly induced in aged seeds after 6–24 h imbibition. In addition, *AsGR2-D* expression was induced by CuSO₄ at 24 h and 36 h. However, the abundance of *AsGR2-D* under cold, PEG, salt, CuSO₄, and H₂O₂ treatments at 72 h was significantly lower (Figure 9D).

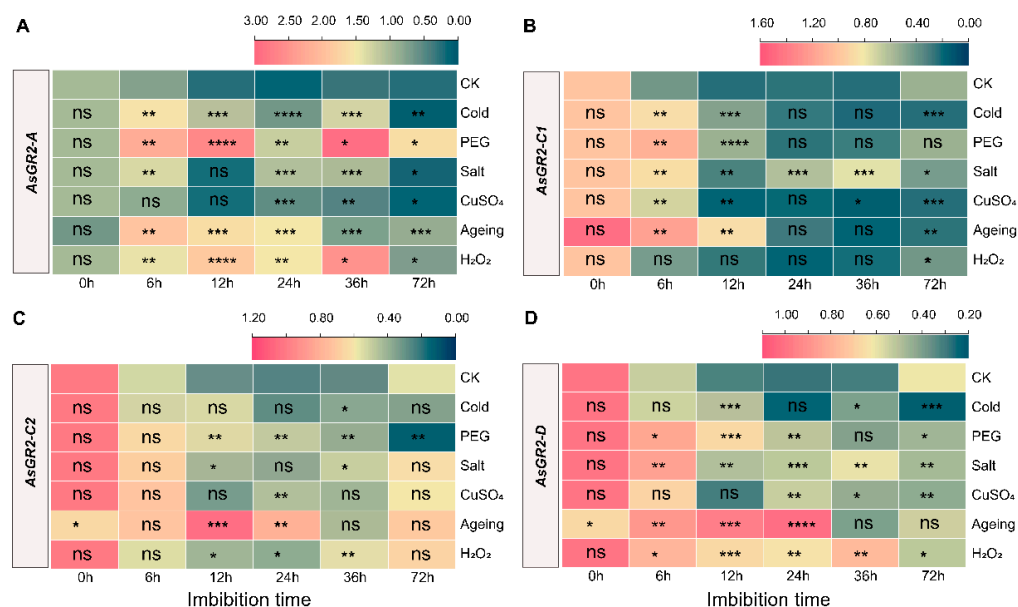


Figure 9. Expression profiling of *AsGR2-A* (A), *AsGR2-C1* (B), *AsGR2-C2* (C), and *AsGR2D* (D) during seed imbibition of *A. sativa* under stress by qPCR. The relative expression was calculated using transcription level of dry seed of CK as reference. The significant expression change in comparison to normal conditions (CK) has been calculated using Student's *t* test. * indicates a significant difference at $p < 0.05$; ** indicates a significant difference at $p < 0.01$; *** indicates a significant difference at $p < 0.001$; **** indicates a significant difference at $p < 0.0001$; ns represents not significant.

3. Discussion

Abiotic stresses, such as drought, salt, cold, heavy metals, and seed ageing, severely affect seed emergence rate and seedling uniformity after sowing. Under adverse conditions, seed germination and seedling growth are inhibited due to the oxidative damage of biomolecules and organelle structures [13,28–30]. In addition, seed ageing, which happens inevitably during seed storage, was also found to be mainly caused by accumulating of excessive ROS [31,32]. GSH plays a crucial role in controlling cellular redox homeostasis, and participates in the elimination of excess ROS under adverse conditions. It is indispensable for the earliest metabolic events during seed germination and maintenance of seed vigor [14]. The level of GSH was suggested to be a promising indicator for seed germination and seedling growth, and was correlated with seed longevity [33,34]. GR is considered to be a crucial enzyme that works on the catalytic reduction of GSSG to the reduced GSH form, thereby involving in plant stress resistance, seed vigor maintenance, growth, and development. Genome-wide identification of the GR proteins has been carried out in *Arabidopsis*, rice, wheat, *B. distachyon*, sorghum, Chinese cabbage and other species, and GRs were divided into cytoplasmic isoform and chloroplast/mitochondrial double-localization isoform. Loss of the two types of GR could decrease plant resistance to adversity [14,35,36], and stresses could also induce GR gene expression and increase GR activity [16,17,37]. However, GR family members in *A. sativa* have not been identified and analyzed systematically. In this study, we identified *A. sativa* GR family members from the whole genome of oat and analyzed their expression patterns during germination under

stress. These gene candidates are useful for the following researches on oat stress resistance breeding and seed vigor improvement.

A total of seven GR proteins were identified in *A. sativa*, which is the same number as that in bread wheat and more than those in other species. It suggested that the GR family members are closely related to their genome duplication events and genome size [24]. GR proteins were initially classified into cytosolic and chloroplast types based on the presence of a typical chloroplast signal peptide at the N-terminus. The AsGR family members were also divided into two clades and were consistent with the predicted subcellular localization. AsGR2-C2 in the chloroplast clade showed a deletion of 230 amino acids at the N-terminus, which may affect its localization and functions. Moreover, GR3 isoform was found in rice, *B. distachyon*, and sorghum, but does not appear in *A. sativa* and bread wheat [24,37]. It suggested that the evolution of GR genes in monocots is complicated. Additionally, *AtGR1* and *AtGR2* of *Arabidopsis* have several homologous in *A. sativa*, wheat and rice, which suggests that the evolutionary divergence of GR genes occurs after the split of monocotyledon and dicotyledon [38].

To understand the structure consistence and divergence of GR proteins, the gene structures and functional motifs of AsGR members were analyzed. The exon-intron patterns of AsGR genes showed that chloroplastic GR genes consisted of fewer exons as compared to cytosolic GR genes, which was highly consistent with the those of *T. aestivum*, *Ae. tauschii*, *B. distachyon*, *S. bicolor*, *B. juncea*, *B. rapa*, etc. [17,24]. However, the exon number of AsGR genes were more than those in most of the other species, which might be due to exon gain, insertion, and exonization during plant evolution [39]. Previous studies have indicated the higher number of exon/intron of cytosolic GR genes might be associated with its expression level [17]. Introns also have been shown to increase transcriptional efficiency of numerous genes in a variety of organisms [40]. Moreover, genes with multiple exons and introns can form more variable splicing isoforms and participate in different regulatory networks. Briefly, the structural changes of GR genes in oat play an important role in its subcellular expression and transcriptional regulation to cope with adverse environment. A total of 15 motifs were discovered in 7 AsGR proteins, which was consistent with bread wheat and *B. distachyon* [24], but less than 19 motifs in Chinese cabbage, *Brassica rapa*, and *Brassica napus* [16,17]. In most cases, chloroplastic GRs showed more motifs than cytosolic isoforms, and several specific motifs can be found in chloroplastic GRs [24]. In the present investigation, motif 10 associated with the N-terminal targeting signal peptide was found in AsGR2-A, AsGR2-C1 and AsGR2-D and showed high identify with chloroplastic signal peptide of TaGRs and OsGRs [15,24]. Previous studies have found that alanine was the most abundant amino acid in monocot transit peptides, whereas serine was the most abundant in eudicot genotypes. In eudicots, serine was more abundant with 30% more serine on average compared with monocot transit peptides [41]. The serine ratio of chloroplast signal peptide in AsGR proteins was 5.9%, which was significantly lower than that of *Arabidopsis* (27.9%). Additionally, motif 12 and motif 13 are specific to AsGR2 and AsGR1, respectively. Motif 14 is at the N- and C- terminals in AsGR1 and AsGR2, respectively. This divergence might be associated with their biochemical activity and functional diversity, as cytosolic, chloroplastic, and mitochondrial GR isoforms showed great difference in catalytic activity [23,42].

Expression profiling is important for understanding gene functions and screening of candidate genes. Genes specifically expressed in different tissues often have specific functions as well. *AsGR1-A* and *AsGR1-C* were highly expressed in non-imbibed seeds, roots, and leaves, and might have a pivotal role in oxidative stress in these tissues. Similarly, the cytosolically localized BcGR1.1 in Chinese cabbage was highly expressed in the roots, and BcGR1.1-overexpressing *Arabidopsis* showed less damage to the root system under copper stress [16]. The cytosolic isoforms in bread wheat (*TaGR2-A*, *TaGR2-B1*, *TaGR2-B2* and *TaGR2-D*), rice (*OsGR2*) and *Arabidopsis* (*AtGR1*) were also highly expressed in root [15,24]. On the other hand, chloroplast/mitochondrial double-localization AsGR2 isoforms were expressed strongly in leaves, lemmas, and dry seeds. Chloroplastic GRs

has been confirmed to be highly expressed in leaves and have the function of maintaining leaf function and coping with senescence [22]. As lemmas were reported to contribute on seed filling especially under adverse conditions, high expression of GR may act on the protection of photosynthetic system in lemmas [43]. In plants, mitochondria and chloroplasts are the main source of ROS. At the later stage of seed development, seeds are subjected to dehydration stress and may have the risk of excessive accumulation of ROS [44]. *TaGR1-B* and *TaGR1-A* were found upregulated at this stage, which would be conducive to alleviating the excessive accumulation of ROS in seeds. High expression levels of *AsGR2* genes were detected in dry *A. sativa* seeds, which might be beneficial for maintaining seed longevity.

The positive role of GR genes in coping with stress has been widely reported. The deletion and low expression of GR genes are often associated with poor stress resistance, while overexpression of GR improves the capacity to withstand oxidative damage caused by abiotic stresses [16,20,23,45]. Expression profiling indicated *AsGR* genes were significantly induced during seed germination under drought stress, especially in the early stage of imbibition, and *AsGR2* genes were more remarkable. This may be considerable for the special biological process of seed germination, since highly reduced GSH pools are needed in the early stage of seed imbibition, so as to alleviate the accumulation of ROS under strong respiration and display the reduction modification of proteins required for germination [11,14]. *AsGR* genes showed diverse responses to salt treatment during germination. The functions of GR genes under salt stress have been well characterized in wheat, tomato, rice, *Stipa purpurea*, and other species [24,36,37,46]. It was reported that salt stress inhibited radicle elongation during seed germination of *A. sativa*, wheat, and rice, while cytoplasmic GR isoforms are highly expressed in roots, which may have a significant protective effect on radicle elongation [47,48]. Under H₂O₂ treatment, *AsGR1-A*, *AsGR1-D*, *AsGR2-A*, and *AsGR2-D* expressions were strongly induced during seed imbibition, indicating that they have more significant effects on protection against oxidative damage, and stress specific induction may exist for *AsGR* genes. Seed ageing is an inevitable and complex process, and its mechanisms have not been well revealed so far. The deletion of chloroplast specific GR2 leads to the embryo lethality, while lack of mitochondrial GR2 leads to a partially oxidized glutathione pool and decreased seed ageing resistance of *Arabidopsis* [14,21]. In addition, our previous study found that the expression of *GR1* in aged *A. sativa* seed embryos (aged from 24 d to 42 d) decreased by 50%–70% compared with the control after imbibition for 24 h and that *GR2* levels decreased significantly in minorly and moderately aged seeds, but were raised significantly in severely aged seeds [33]. In present study, the expression of *AsGR2-C2* and *AsGR2-D* decreased significantly in dry seeds after ageing treatment, but they increased rapidly in the early stage of imbibition. Ageing may cause damage to the mitochondrial structural and functional systems [13,30,49]. In the early stage of seed imbibition, excessive respiration can increase the electron transport of mitochondria, which will lead to electron leakage and ROS accumulation [6]. In this study, the expression of *AsGR2-A*, *AsGR2-C1*, and *AsGR2-D* was highly expressed in the early stage of seed imbibition, which could alleviate the damaged redox homeostasis in mitochondria and ensure the energy supply for seed germination. It is suggested that *AsGR2* might be more active on the maintenance of redox homeostasis during germination, especially under PEG, ageing, and H₂O₂ stress.

Cis-regulatory elements in the promoters control development and physiology by regulating gene expression. Hormone and stress responsive elements are the main functional factors detected in the promoters of *AsGR* genes. This study analyzed the expression of *AsGR* genes under stress during seed germination, but the response of *AsGR* genes to hormone should also be concerned. The crosstalk of hormonal and redox signals has been demonstrated to play a pivotal role in the regulation of plant resistance, leaf senescence, seed germination, seed development, and seed longevity [50–52]. Plant growth and environmental adaptation are regulated by various combinations of *cis*-elements, and only a small set of responsive genes can be regulated by a single *cis*-element [53]. GA, ABA, SA,

MeJA, and IAA responsive elements combined with stress responsive elements may play an important role in the regulation of stress resistance and development. Moreover, these *cis*-elements seem to be species-specific and subcellular localization-specific. For instance, ABA-responsive elements were not found in the promoter of pea GR genes [54], but only in the promoter of *AsGR2* genes and not in the promoter of *AsGR1* genes in *A. sativa*. ABA is a crucial factor of seed vigor, and it has been found to play a regulatory role in mitochondrial ROS production and energy metabolism in recent years [55,56]. It is hypothesized that the interaction between mitochondrial GR2 and ABA may play a role in regulating seed vigor. Consequently, the regulatory relationship between *AsGR2* genes and hormone signaling should be focused on in the future.

4. Materials and Methods

4.1. Identification and Chromosomal Location of *AsGR* Genes

The genome information of *A. sativa* and its possible ancestors *A. longiglumis* and *A. insularis* were downloaded from the GrainGenes database (<https://wheat.pw.usda.gov/GG3/>, accessed on 24 November 2021). The rice GR proteins (LOC_Os02g56850.1, LOC_Os03g06740.1 and LOC_Os10g28000.1) and *Arabidopsis* GR proteins (AT3G24170 and AT3G54660) were used as query sequences to obtain possible GR proteins in three genomes by BlastP search with a cutoff e-value of $1 \times e^{-5}$. Further, the predicted GR protein sequences were reconfirmed by Simple Modular Architecture Research Tool (SMART; <http://smart.embl-heidelberg.de/smart/batch.pl>, accessed on 26 February 2022), Pfam (<http://pfam.xfam.org/>, accessed on 26 February 2022), and NCBI conserved domain database (<https://www.ncbi.nlm.nih.gov/>, accessed on 26 February 2022) [24,57]. Chromosomal location of oat GR members was displayed by TBtools. For nomenclature, *AsGR* genes were named according to wheat GR genes, which referenced the international rule for wheat gene symbolization (<http://wheat.pw.usda.gov/ggpages/wgc/98/Intro.htm>, accessed on 16 February 2022) and presented the chromosomal information of GR members.

4.2. Physiochemical Properties and Subcellular Localization

The physical and chemical properties of *A. sativa* GR proteins were analyzed by using the online program ExPaSy-ProtParam (<https://web.expasy.org/protparam/>, accessed on 16 March 2022), including amino acids (AA) number, molecular weight (MW), theoretical isoelectric points (pI), etc. Protein subcellular localization prediction was performed using the online tools WoLF PSORT (<https://wolfpsort.hgc.jp/>, accessed on 28 March 2022), CELLO v.2.5 (<http://cello.life.nctu.edu.tw/>, accessed on 28 March 2022), and Cell-PLoc 2.0 (<http://www.csbio.sjtu.edu.cn/bioinf/Cell-PLoc-2/>, accessed on 28 March 2022).

4.3. Phylogenetic Analysis of GR Proteins of Oat and Other Plant Species

The identified GR proteins were used to conduct multiple sequence alignment with GR members derived from *Arabidopsis*, rice and bread wheat by ClustalX2 software with the default parameters [58]. Phylogenetic tree was constructed using the sequence alignment results with the neighbor-joining (NJ) method in MEGA6.0 [59]. The bootstrap was tested 10,000 times and expressed as a percentage of 1000 replicates.

4.4. Motif Pattern and Gene Structure Analysis of *AsGR* Members

GR protein sequences were used to predict the occurrence of functional motifs in the MEME website (<http://meme-suite.org/>, accessed on 19 February 2022). TBtools ver 1.0986 were used to edit the motif pattern and gene structure diagrams [60].

4.5. Multiple Sequence Alignment and Homology Modelling of *AsGR* Proteins

Multiple sequence alignment of *AsGRs* with already known GRs from *Arabidopsis thaliana* (AtGR1 and AtGR2), was performed using ClustalX2 software and visualized using GeneDoc software [58]. The conserved domain and targeting signal peptides which are essential in redox activity and subcellular localization are boxed according to previous

description [17,23]. All of the AsGR members were three-dimensionally modeled using the Phyre2 server (<http://www.sbg.bio.ic.ac.uk/phyre2/html/>, accessed on 2 April 2022) [61]. The topmost hit crystal structure of putative glutathione reductase from *Sinorhizobium meliloti* 1021 (PDB: 4DNA) chain A was used as a template.

4.6. Identification of Cis-Elements in the Promoter Region of AsGR Genes

In order to determine the responses of AsGR genes to stress treatments, we retrieved 2 kb of the deduced promoter region from *A. sativa* genome database to identify the cis-regulatory elements using PlantCARE [62].

4.7. Plant Material, Treatment and Collection of Tissues

Oat (cv Challenger) seeds with germination percentage of 100% were used in the present study. For *A. sativa* tissue-specific expression profiling of AsGRs, twelve samples including seeds, roots, leaves, stems, florets and lemmas were used. In detail, seed samples were collected in imbibition phases (imbibition for 0 h, 12 h and 24 h) and development phases (8, 15 and 30 days after flowering, DAF). Young leaves, lemmas and florets were collected at flowering stage, and old leaves were from plants at 30 DAF. The roots were obtained from 10-day-old plants. To understand the expression profiling of AsGRs during seed germination under salt, drought and heavy metal stresses, seeds were subjected to 150 mM NaCl, 20% PEG 6000 and 200 mg L⁻¹ CuSO₄·5H₂O solution for imbibition, respectively [63–66]. For oxidative stress, seeds were imbibed in 2% H₂O₂, since the germination percentage decreased from almost 100% to 45% after treatment. For control, cold treatment and ageing treatment, seeds were imbibed in distilled water. Seed ageing treatment were according to Xia et al. [13], and seeds ageing time was according to our previous investigation [33]. Cold treatment was carried out at 10 °C, while control and other treatments were imbibed at 20 °C in the plant growth incubator under 16 h dark and 8 h light cycle. Seed samples were collected after imbibition for 0 h, 6 h, 12 h, 24 h, 36 h and 72 h, which included the three major phases of oat seed imbibition under normal conditions. Each tissue sample contained three biological replicates, and each replicate was collected from at least ten seeds or plants. The collected tissue samples were then ground into powder in liquid nitrogen.

4.8. qRT-PCR and Statistical Analyses of AsGR Genes

Total RNA was extracted using Quick RNA isolation Kit (Huayueyang Biotech Co., Ltd., Beijing, China). First-strand cDNA was synthesized from 1 µg RNA using EasyScript[®] All-in-One First-Strand cDNA Synthesis SuperMix for qPCR Kit (TransGen Biotech, Beijing, China). qRT-PCR analysis was performed on a CFX96 Real-Time System (Bio-Rad, Hercules, CA, USA) using 2×RealStar Green Fast Mixture (Genstar, China) with *AsEIF4A* gene as reference gene [67]. The thermal cycle program was 95 °C for 25 min, and 40 cycles of 95 °C for 5 s and 60 °C for 10 s. The comparative delta-Ct method was used to calculate the relative transcript levels of AsGR genes [68]. The comparison of relative expression level between different tissues were performed in SPSS Statistics 22 using ANOVA and a Duncan's test, and visualized using GraphPad Prism version 8.0. The expression heatmaps of AsGR genes during seed imbibition under stress were visualized using TBtools ver 1.0986. The significant expression change in comparison to normal conditions was calculated using Student's *t* test. The details of the primers used in qRT-PCR assay are listed in Table S1.

5. Conclusions

In summary, seven AsGR genes were identified and mapped on six chromosomes of A, C and D subgenomes. Phylogenetic analysis and subcellular localization of AsGR proteins suggested they were divided in two sub-families, AsGR1 and AsGR2, which showed predicted subcellular location of cytoplasm and chloroplast/mitochondrion, respectively. Structure analysis suggested AsGR genes were highly conserved and that AsGR1 contained higher number of exon/introns. Both AsGR1 and AsGR2 genes have relatively high expres-

sion in leaves and dry seeds, suggesting they may play a role in maintaining leaf function and seed vigor. Their responses to drought, salt, cold, copper, H₂O₂, and ageing treatments were quite different during seed imbibition. Among the seven *AsGR* genes, *AsGR1-A*, *AsGR1-C*, *AsGR2-A*, and *AsGR2-D* responded more significantly, especially under drought, ageing, and H₂O₂ stress. It suggested that they might be more active on the maintenance of redox homeostasis during seed imbibition under unfavorable conditions. The present study will lay the foundation for future studies on verifications of the precise regulation of *GR* genes in *A. sativa*. Finally, stress-responsive *AsGR* genes can be used for genetic improvement of stress resistance and seed vigor in oat.

Supplementary Materials: The following supporting information can be downloaded at: <https://www.mdpi.com/article/10.3390/ijms231911650/s1>.

Author Contributions: Conceptualization, P.M. and M.S.; methodology, M.S. and S.S.; software, M.S., S.S., Z.J. and H.Z.; validation, M.S. and S.S.; formal analysis, M.S. and S.S.; investigation, M.S., Z.J., W.M., C.M., C.O., L.H. and J.W.; resources, P.M.; data curation, M.S. and Z.J.; writing—original draft preparation, M.S.; writing—review and editing, P.M., M.L. and S.J.; visualization, M.S.; supervision, P.M. and S.J.; project administration, P.M.; funding acquisition, P.M. All authors have read and agreed to the published version of the manuscript.

Funding: This research was funded by the earmarked fund for China Agriculture Research System (CARS-34 to P.M.).

Institutional Review Board Statement: Not applicable.

Informed Consent Statement: Not applicable.

Data Availability Statement: Data is contained within the article and supplementary material.

Conflicts of Interest: The authors declare no conflict of interest.

References

1. Mhamdi, A.; Van Breusegem, F. Reactive oxygen species in plant development. *Development* **2018**, *145*, dev164376. [[CrossRef](#)] [[PubMed](#)]
2. Consideine, M.J.; Foyer, C.H. Oxygen and reactive oxygen species-dependent regulation of plant growth and development. *Plant Physiol.* **2021**, *186*, 79–92. [[CrossRef](#)] [[PubMed](#)]
3. Waszczak, C.; Carmody, M.; Kangasjarvi, J. Reactive oxygen species in plant signaling. *Annu. Rev. Plant Biol.* **2018**, *69*, 209–236. [[CrossRef](#)] [[PubMed](#)]
4. Czarnocka, W.; Karpinski, S. Friend or foe? Reactive oxygen species production, scavenging and signaling in plant response to environmental stresses. *Free Radic. Biol. Med.* **2018**, *122*, 4–20. [[CrossRef](#)] [[PubMed](#)]
5. Zhou, W.; Chen, F.; Luo, X.; Dai, Y.; Yang, Y.; Zheng, C.; Yang, W.; Shu, K. A matter of life and death: Molecular, physiological, and environmental regulation of seed longevity. *Plant Cell Environ.* **2020**, *43*, 293–302. [[CrossRef](#)]
6. Bailly, C. Active oxygen species and antioxidants in seed biology. *Seed Sci. Res.* **2007**, *14*, 93–107. [[CrossRef](#)]
7. Hasanuzzaman, M.; Bhuyan, M.; Anee, T.I.; Parvin, K.; Nahar, K.; Mahmud, J.A.; Fujita, M. Regulation of ascorbate-glutathione pathway in mitigating oxidative damage in plants under abiotic stress. *Antioxidants* **2019**, *8*, 384. [[CrossRef](#)]
8. Hasanuzzaman, M.; Nahar, K.; Anee, T.I.; Fujita, M. Glutathione in plants: Biosynthesis and physiological role in environmental stress tolerance. *Physiol. Mol. Biol. Plants* **2017**, *23*, 249–268. [[CrossRef](#)]
9. Foyer, C.H.; Noctor, G. Ascorbate and glutathione: The heart of the redox hub. *Plant Physiol.* **2011**, *155*, 2–18. [[CrossRef](#)]
10. Gill, S.S.; Anjum, N.A.; Hasanuzzaman, M.; Gill, R.; Trivedi, D.K.; Ahmad, I.; Pereira, E.; Tuteja, N. Glutathione and glutathione reductase: A boon in disguise for plant abiotic stress defense operations. *Plant Physiol. Biochem.* **2013**, *70*, 204–212. [[CrossRef](#)]
11. Tommasi, F.; Paciolla, C.; de Pinto, M.C.; Gara, L.D. A comparative study of glutathione and ascorbate metabolism during germination of *Pinus pinea* L. seeds. *J. Exp. Bot.* **2001**, *52*, 1647–1654. [[CrossRef](#)]
12. Pei, L.; Che, R.; He, L.; Gao, X.; Li, W.; Li, H. Role of exogenous glutathione in alleviating abiotic stress in maize (*Zea mays* L.). *J. Plant Growth Regul.* **2018**, *38*, 199–215. [[CrossRef](#)]
13. Xia, F.; Cheng, H.; Chen, L.; Zhu, H.; Mao, P.; Wang, M. Influence of exogenous ascorbic acid and glutathione priming on mitochondrial structural and functional systems to alleviate aging damage in oat seeds. *BMC Plant Biol.* **2020**, *20*, 104. [[CrossRef](#)] [[PubMed](#)]
14. Nietzel, T.; Mostertz, J.; Ruberti, C.; Née, G.; Fuchs, P.; Wagner, S.; Moseler, A.; Müller-Schüssele, S.J.; Benamar, A.; Poschet, G.; et al. Redox-mediated kick-start of mitochondrial energy metabolism drives resource-efficient seed germination. *Proc. Natl. Acad. Sci. USA* **2020**, *117*, 741. [[CrossRef](#)]

15. Trivedi, D.K.; Gill, S.S.; Yadav, S.; Tuteja, N. Genome-wide analysis of glutathione reductase (GR) genes from rice and *Arabidopsis*. *Plant Signal Behav.* **2013**, *8*, e23021. [[CrossRef](#)]
16. Li, Y.; Huang, F.; Tao, Y.; Zhou, Y.; Bai, A.; Yu, Z.; Xiao, D.; Zhang, C.; Liu, T.; Hou, X.; et al. BcGR1.1, a cytoplasmic localized glutathione reductase, enhanced tolerance to copper stress in *Arabidopsis thaliana*. *Antioxidants* **2022**, *11*, 389. [[CrossRef](#)] [[PubMed](#)]
17. Verma, D.; Singh, K. Understanding role of glutathione reductase gene family in drought and heat stresses in *Brassica juncea* and *B. rapa*. *Environ. Exp. Bot.* **2021**, *190*, 104595. [[CrossRef](#)]
18. Contour-Ansel, D.; Torres-Franklin, M.L.; Cruz, D.E.C.M.H.; D'Arcy-Lameta, A.; Zuily-Fodil, Y. Glutathione reductase in leaves of cowpea: Cloning of two cDNAs, expression and enzymatic activity under progressive drought stress, desiccation and abscisic acid treatment. *Ann. Bot.* **2006**, *98*, 1279–1287. [[CrossRef](#)]
19. Ma, Y.; Ma, F.; Zhang, J.; Li, M.; Wang, Y.; Liang, D. Effects of high temperature on activities and gene expression of enzymes involved in ascorbate–glutathione cycle in apple leaves. *Plant Sci.* **2008**, *175*, 761–766. [[CrossRef](#)]
20. Pilon-Smits, E.A.H.; Zhu, Y.L.; Sears, T.; Terry, N. Overexpression of glutathione reductase in *Brassica juncea*: Effects on cadmium accumulation and tolerance. *Physiol Plant.* **2000**, *110*, 455–460. [[CrossRef](#)]
21. Marty, L.; Bausewein, D.; Müller, C.; Bangash, S.A.K.; Moseler, A.; Schwarzländer, M.; Müller-Schüssele, S.J.; Zechmann, B.; Riondet, C.; Balk, J.; et al. *Arabidopsis* glutathione reductase 2 is indispensable in plastids, while mitochondrial glutathione is safeguarded by additional reduction and transport systems. *New Phytol.* **2019**, *224*, 1569–1584. [[CrossRef](#)]
22. Ding, S.; Wang, L.; Yang, Z.; Lu, Q.; Wen, X.; Lu, C. Decreased glutathione reductase2 leads to early leaf senescence in *Arabidopsis*. *J. Integr. Plant Biol.* **2016**, *58*, 29–47. [[CrossRef](#)]
23. Liu, H.J.; Wang, X.; Yang, Z.L.; Ren, L.L.; Qian, T.T. Identification and biochemical characterization of the glutathione reductase family from *Populus trichocarpa*. *Plant Sci.* **2020**, *294*, 110459. [[CrossRef](#)]
24. Madhu; Kaur, A.; Tyagi, S.; Singh, K.; Upadhyay, S.K. Exploration of glutathione reductase for abiotic stress response in bread wheat (*Triticum aestivum* L.). *Plant Cell Rep.* **2022**, *41*, 639–654. [[CrossRef](#)] [[PubMed](#)]
25. Rasane, P.; Jha, A.; Sabikhi, L.; Kumar, A.; Unnikrishnan, V.S. Nutritional advantages of oats and opportunities for its processing as value added foods—a review. *J. Food Sci. Technol.* **2015**, *52*, 662–675. [[CrossRef](#)] [[PubMed](#)]
26. Kamal, N.; Tsardakas Renhuldt, N.; Bentzer, J.; Gundlach, H.; Haberer, G.; Juhasz, A.; Lux, T.; Bose, U.; Tye-Din, J.A.; Lang, D.; et al. The mosaic oat genome gives insights into a uniquely healthy cereal crop. *Nature* **2022**, *606*, 113–119. [[CrossRef](#)] [[PubMed](#)]
27. Peng, Y.; Yan, H.; Guo, L.; Deng, C.; Wang, C.; Wang, Y.; Kang, L.; Zhou, P.; Yu, K.; Dong, X.; et al. Reference genome assemblies reveal the origin and evolution of allohexaploid oat. *Nat. Genet.* **2022**, *54*, 1248–1258. [[CrossRef](#)]
28. Rajjou, L.; Duval, M.; Gallardo, K.; Catusse, J.; Bally, J.; Job, C.; Job, D. Seed germination and vigor. *Annu. Rev. Plant Biol.* **2012**, *63*, 507–533. [[CrossRef](#)] [[PubMed](#)]
29. Bailly, C.; Merendino, L. Oxidative signalling in seed germination and early seedling growth: An emerging role for ROS trafficking and inter-organelle communication. *Biochem. J.* **2021**, *478*, 1977–1984. [[CrossRef](#)] [[PubMed](#)]
30. Ratajczak, E.; Malecka, A.; Ciereszko, I.; Staszak, A.M. Mitochondria are important determinants of the aging of seeds. *Int. J. Mol. Sci.* **2019**, *20*, 1568. [[CrossRef](#)]
31. Kurek, K.; Plitta-Michalak, B.; Ratajczak, E. Reactive oxygen species as potential drivers of the seed aging process. *Plants* **2019**, *8*, 174. [[CrossRef](#)] [[PubMed](#)]
32. Bailly, C.; Kranner, I. Analyses of reactive oxygen species and antioxidants in relation to seed longevity and germination. *Methods Mol. Biol.* **2011**, *773*, 343–367.
33. Sun, M.; Sun, S.; Mao, C.; Zhang, H.; Ou, C.; Jia, Z.; Wang, Y.; Ma, W.; Li, M.; Jia, S.; et al. Dynamic responses of antioxidant and glyoxalase systems to seed aging based on full-length transcriptome in oat (*Avena sativa* L.). *Antioxidants* **2022**, *11*, 395. [[CrossRef](#)]
34. Ninoles, R.; Planes, D.; Arjona, P.; Ruiz-Pastor, C.; Chazarra, R.; Renard, J.; Bueso, E.; Forment, J.; Serrano, R.; Kranner, I.; et al. Comparative analysis of wild-type accessions reveals novel determinants of *Arabidopsis* seed longevity. *Plant Cell Environ.* **2022**, *45*, 2708–2728. [[CrossRef](#)]
35. Mhamdi, A.; Hager, J.; Chaouch, S.; Queval, G.; Han, Y.; Tacconat, L.; Saindrenan, P.; Gouia, H.; Issakidis-Bourguet, E.; Renou, J.P.; et al. *Arabidopsis* glutathione reductase1 plays a crucial role in leaf responses to intracellular hydrogen peroxide and in ensuring appropriate gene expression through both salicylic acid and jasmonic acid signaling pathways. *Plant Physiol.* **2010**, *153*, 1144–1160. [[CrossRef](#)]
36. Wu, T.M.; Lin, W.R.; Kao, C.H.; Hong, C.Y. Gene knockout of glutathione reductase3 results in increased sensitivity to salt stress in rice. *Plant Mol. Biol.* **2015**, *87*, 555–564. [[CrossRef](#)] [[PubMed](#)]
37. Wu, T.M.; Lin, W.R.; Kao, Y.T.; Hsu, Y.T.; Yeh, C.H.; Hong, C.Y.; Kao, C.H. Identification and characterization of a novel chloroplast/mitochondria co-localized glutathione reductase 3 involved in salt stress response in rice. *Plant Mol. Biol.* **2013**, *83*, 379–390. [[CrossRef](#)] [[PubMed](#)]
38. Kirst, M.; Johnson Arthur, F.; Baucom, C.; Ulrich, E.; Hubbard, K.; Staggs, R.; Paule, C.; Retzel, E.; Whetten, R.; Sederoff, R. Apparent homology of expressed genes from wood-forming tissues of loblolly pine (*Pinus taeda* L.) with *Arabidopsis thaliana*. *Proc. Natl. Acad. Sci. USA* **2003**, *100*, 7383–7388. [[CrossRef](#)]
39. Xu, G.; Guo, C.; Shan, H.; Kong, H. Divergence of duplicate genes in exon-intron structure. *Proc. Natl. Acad. Sci. USA* **2012**, *109*, 1187–1192. [[CrossRef](#)]
40. Le Hir, H.; Nott, A.; Moore, M.J. How introns influence and enhance eukaryotic gene expression. *Trends Biochem. Sci.* **2003**, *28*, 215–220. [[CrossRef](#)]

41. Christian, R.W.; Hewitt, S.L.; Nelson, G.; Roalson, E.H.; Dhingra, A. Plastid transit peptides—where do they come from and where do they all belong? Multi-genome and pan-genomic assessment of chloroplast transit peptide evolution. *PeerJ* **2020**, *8*, e9772. [[CrossRef](#)] [[PubMed](#)]
42. Stevens, R.G.; Creissen, G.P.; Mullineaux, P.M. Cloning and characterisation of a cytosolic glutathione reductase cDNA from pea (*Pisum sativum* L.) and its expression in response to stress. *Plant Mol. Biol.* **1997**, *35*, 641–654. [[CrossRef](#)]
43. Abebe, T.; Melmaiee, K.; Berg, V.; Wise, R.P. Drought response in the spikes of barley: Gene expression in the lemma, palea, awn, and seed. *Funct. Integr. Genom.* **2010**, *10*, 191–205. [[CrossRef](#)]
44. Dinakar, C.; Djilianov, D.; Bartels, D. Photosynthesis in desiccation tolerant plants: Energy metabolism and antioxidative stress defense. *Plant Sci.* **2012**, *182*, 29–41. [[CrossRef](#)]
45. Foyer, C.H.; Souriau, N.; Perret, S.; Lelandais, M.; Kunert, K.J.; Pruvost, C.; Jouanin, L. Overexpression of glutathione reductase but not glutathione synthetase leads to increases in antioxidant capacity and resistance to photoinhibition in poplar trees. *Plant Physiol.* **1995**, *109*, 1047–1057. [[CrossRef](#)] [[PubMed](#)]
46. Wang, Q.; Pu, Y.; Yang, D.; Yin, X.; He, Z.; Yang, Y.; Yang, Y. Molecular cloning and characterization of the glutathione reductase gene from *Stipa purpurea*. *Biochem. Biophys. Res. Commun.* **2018**, *495*, 1851–1857. [[CrossRef](#)] [[PubMed](#)]
47. Luo, X.; Han, C.; Deng, X.; Zhu, D.; Liu, Y.; Yan, Y. Identification of phosphorylated proteins in response to salt stress in wheat embryo and endosperm during seed germination. *Cereal Res. Commun.* **2019**, *47*, 53–66. [[CrossRef](#)]
48. Kamyar, K. Effects of salt stress on germination and early seedling growth of rice (*Oryza sativa*) cultivars in Iran. *Afr. J. Biotechnol.* **2011**, *10*, 17789–17792. [[CrossRef](#)]
49. Li, Y.; Wang, Y.; Xue, H.; Pritchard, H.W.; Wang, X. Changes in the mitochondrial protein profile due to ROS eruption during ageing of elm (*Ulmus pumila* L.) seeds. *Plant Physiol. Biochem.* **2017**, *114*, 72–87. [[CrossRef](#)]
50. Jurdak, R.; Launay-Avon, A.; Paysant-Le Roux, C.; Bailly, C. Retrograde signalling from the mitochondria to the nucleus translates the positive effect of ethylene on dormancy breaking of *Arabidopsis thaliana* seeds. *New Phytol.* **2021**, *229*, 2192–2205. [[CrossRef](#)]
51. Bailly, C. The signalling role of ROS in the regulation of seed germination and dormancy. *Biochem. J.* **2019**, *476*, 3019–3032. [[CrossRef](#)] [[PubMed](#)]
52. Zimmermann, P.; Zentgraf, U. The correlation between oxidative stress and leaf senescence during plant development. *Cell. Mol. Biol. Lett.* **2005**, *10*, 515. [[PubMed](#)]
53. Zou, C.; Sun, K.; Mackaluso, J.D.; Seddon, A.E.; Jin, R.; Thomashow, M.F.; Shiu, S.H. Cis-regulatory code of stress-responsive transcription in *Arabidopsis thaliana*. *Proc. Natl. Acad. Sci. USA* **2011**, *108*, 14992–14997. [[CrossRef](#)] [[PubMed](#)]
54. Harshvardhan, V.T.; Wu, T.M.; Hong, C.Y. Glutathione reductase and abiotic stress tolerance in plants. In *Glutathione in Plant Growth, Development, and Stress Tolerance*; Hossain, M.A., Mostofa, M.G., Diaz-Vivancos, P., Burritt, D.J., Fujita, M., Tran, L.S.P., Eds.; Springer International Publishing: Cham, Switzerland, 2017; pp. 265–286.
55. Huang, S.; Van Aken, O.; Schwarzlander, M.; Belt, K.; Millar, A.H. The roles of mitochondrial reactive oxygen species in cellular signaling and stress response in plants. *Plant Physiol.* **2016**, *171*, 1551–1559. [[CrossRef](#)] [[PubMed](#)]
56. Wagner, S.; Van Aken, O.; Elsasser, M.; Schwarzlander, M. Mitochondrial energy signaling and its role in the low-oxygen stress response of plants. *Plant Physiol.* **2018**, *176*, 1156–1170. [[CrossRef](#)]
57. Wang, L.; Bei, X.; Gao, J.; Li, Y.; Yan, Y.; Hu, Y. The similar and different evolutionary trends of MATE family occurred between rice and *Arabidopsis thaliana*. *BMC Plant Biol.* **2016**, *16*, 207. [[CrossRef](#)]
58. Larkin, M.A.; Blackshields, G.; Brown, N.P.; Chenna, R.; McGettigan, P.A.; McWilliam, H.; Valentin, F.; Wallace, I.M.; Wilm, A.; Lopez, R. Clustal W and Clustal X version 2.0. *Bioinformatics* **2007**, *23*, 2947–2948. [[CrossRef](#)]
59. Tamura, K.; Stecher, G.; Peterson, D.; Filipski, A.; Kumar, S. MEGA6: Molecular evolutionary genetics analysis version 6.0. *Mol. Biol. Evol.* **2013**, *30*, 2725–2729. [[CrossRef](#)]
60. Chen, C.; Chen, H.; Zhang, Y.; Thomas, H.R.; Frank, M.H.; He, Y.; Xia, R. TBtools: An integrative toolkit developed for interactive analyses of big biological data. *Mol. Plant* **2020**, *13*, 1194–1202. [[CrossRef](#)]
61. Kelley, L.A.; Mezulis, S.; Yates, C.M.; Wass, M.N.; Sternberg, M.J. The Phyre2 web portal for protein modeling, prediction and analysis. *Nat. Protoc.* **2015**, *10*, 845–858. [[CrossRef](#)]
62. Lescot, M.; Déhais, P.; Thijs, G.; Marchal, K.; Moreau, Y.; Van de Peer, Y.; Rouzé, P.; Rombauts, S. PlantCARE, a database of plant cis-acting regulatory elements and a portal to tools for in silico analysis of promoter sequences. *Nucleic. Acids Res.* **2002**, *30*, 325–327. [[CrossRef](#)] [[PubMed](#)]
63. Xu, Z.; Chen, X.; Lu, X.; Zhao, B.; Yang, Y.; Liu, J. Integrative analysis of transcriptome and metabolome reveal mechanism of tolerance to salt stress in oat (*Avena sativa* L.). *Plant Physiol. Biochem.* **2021**, *160*, 315–328. [[CrossRef](#)]
64. Zhang, M.; Bai, R.; Nan, M.; Ren, W.; Wang, C.; Shabala, S.; Zhang, J. Evaluation of salt tolerance of oat cultivars and the mechanism of adaptation to salinity. *J. Plant Physiol.* **2022**, *273*, 153708. [[CrossRef](#)]
65. Xie, H.; Li, M.; Chen, Y.; Zhou, Q.; Liu, W.; Liang, G.; Jia, Z. Important physiological changes due to drought stress on oat. *Front. Ecol. Evol.* **2021**, *9*, 271. [[CrossRef](#)]
66. Ruan, Y.; Ji, G.; Gao, J.; Ling, L.; Wang, H. Phytochemical and gene expression reveals the antioxidant responses to copper ions in *Brassica rapa*. *J. Plant Growth Regul.* **2020**, *39*, 313–323. [[CrossRef](#)]

-
67. Yang, Z.; Wang, K.; Aziz, U.; Zhao, C.; Zhang, M. Evaluation of duplicated reference genes for quantitative real-time PCR analysis in genome unknown hexaploid oat (*Avena sativa* L.). *Plant Methods* **2020**, *16*, 139. [[CrossRef](#)] [[PubMed](#)]
 68. Jia, S.; Yobi, A.; Naldrett, M.J.; Alvarez, S.; Angelovici, R.; Zhang, C.; Holding, D.R. Deletion of maize RDM4 suggests a role in endosperm maturation as well as vegetative and stress-responsive growth. *J. Exp. Bot.* **2020**, *71*, 5880–5895. [[CrossRef](#)] [[PubMed](#)]